High resolution gratings for the soft x-ray

Michael C. Hettrick

Nucl. Instrum. Meth. Vol. A266, Issues 1-3, pp. 404-413 (1988)

http://dx.doi.org/10.1016/0168-9002(88)90420-2

Nuclear Instruments and Methods in Physics Research A266 (1988) 404–413
North-Holland, Amsterdam

Section III. Beamline instrumentation: (c) Grating monochromators

HIGH RESOLUTION GRATINGS FOR THE SOFT X-RAY

Michael C. HETTRICK *

Hettrick Scientific, P.O. Box 8046, Berkeley, CA 94707, USA

I discuss methods of obtaining high spectral resolution for soft X-ray and extreme ultraviolet radiation employing reflection gratings at grazing incidence. Resolution is optimized when the geometrical aberrations, caused by a large optical aperture, are comparable to the physical diffraction limit. The simplest method of aberration correction, that of under-illuminating the grating, is experimentally shown to result in a great sacrifice in the throughput and only a modest gain in resolution for a fixed slit monochromator employing a conventional spherical grating. The use of a plane grating with varied groove spacing to reduce or eliminate some aberrations is discussed, in the geometry of converging incident radiation. It is shown that spectrometers and monochromators employing such gratings are tunable in wavelength using fixed slits and a fixed beam direction, are spatially stigmatic without sacrifice of spectral resolution, and benefit in practical ways due to spectra which are perpendicular to the diffracted beam. Performances are discussed in the context both of prior results and present experiments using laser produced plasmas, and of future applications using the soft X-ray radiation emitted from synchrotrons.

1. Introduction

Currently, modern synchrotron radiation facilities are being designed and constructed for the exclusive purpose of using the intense short wavelength radiation which can be generated both by bending magnets and by sophisticated insertion devices such as wigglers and undulators [1,2]. These advances in synchrotron design must be accompanied by the use of state-of-the-art monochromators to outfit the beamlines if the user is to take full advantage of such facilities. Among the generally desired properties for such monochromators are: (1) High spectral resolution (resolving powers of 10^4 and higher); (2) high brightness, requiring stigmatic (pointlike) imaging, and (3) a fixed position instrument, easily operable under ultrahigh vacuum.

In this paper, I review how varied-space gratings can be exploited to achieve these requirements simultaneously, while also meeting practical considerations of fabrication and alignment. In section 2 I will sketch the origin of varied-space plane gratings and demonstrate their use as tools for space instrumentation and laboratory soft X-ray spectroscopy. The general approach and experimental results will be briefly discussed. In section 3 I will outline how some aspects of this approach were adapted to the design of a monochromator using simple spherical gratings, thus providing high collection capability and representing a vast improvement over the toroidal grating monochromator which previously dominated high throughput research. In section 4 I will review how the design of a monochromator based on full exploitation of varied-space plane gratings compares in performance to the simpler spherical grating design when both are constrained to operate with fixed slits. In section 5 I conclude this work.

I attempt here to outline an equation-free intuitive approach and to present experimental results which illustrate some useful properties of these designs. For the detailed quantitative analysis governing these properties, the reader should consult the references given here of the original works. Further, I shall address only the instrumentation aspects of these designs, leaving to other works the discussion of particular scientific results obtained.

2. Historical background

Descriptions of varied-space plane gratings for spectroscopy have been published extensively in the literature [3–7]. In fig. 1 I reproduce the basic geometry [3] which is that of a convergent light beam incident onto a plane grating surface. The incident beam is provided by a mirror (not shown) which focuses the radiation to a point. Regardless of the grating groove locations, in zero order reflection the grating will behave as a plane mirror, diverting the mirror focus without aberration to the point denoted $m = 0$. The first order spectrum, composed of various wavelengths, will be dispersed above this point. If the grating grooves are straight and parallel to each other, they will not significantly distort the converging beam in the direction perpendicular to dispersion, hence astigmatism will be zero along the

* Previous affiliation: Center for X-ray Optics, Lawrence Berkeley Laboratory, Berkeley, CA 94720, USA.

0168-9002/88/$03.50

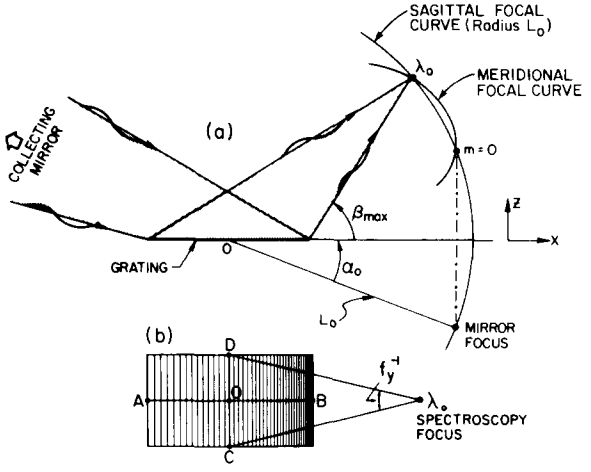

Fig. 1. Mounting geometry of a plane varied-space reflection grating. An upstream optic provides converging radiation, and the grating focuses a spectrum of wavelengths along the meridional curve which, due to the varied groove spacings, is nearly perpendicular to the diffracted rays. Astigmatism is eliminated along the sagittal curve (a circle) which intersects the meridional curve at two points.

sagittal focal curve which is a circle centered at the central groove of the grating.

However, for equally spaced grooves the spectral resolution ($\Delta\lambda/\lambda$), resulting from the size of the wavelength image in the dispersion direction perpendicular to the grating grooves, will be unuseable along this astigmatism-free circle. This is because the spectral focal surface is a lemniscate which at grazing incidence deviates significantly from the sagittal focal surface. Now consider varying the spacings between the grooves, yet keeping them straight and parallel to each other. One can always find a set of such groove locations which will result in perfect constructive interference in first order at a chosen wavelength and a chosen position in two-dimensional space within the dispersion plane above the grating surface. It is clearly advantageous to place this best spectral focus at a position along the sagittal focal circle where astigmatism is also absent, resulting in a point image. Because the zero order image, corresponding to a wavelength of zero, is also a point, it is apparent that first order images of wavelengths other than the chosen one will still be well-focused along the sagittal curve. While the optimum spectral resolution is obtained along a slightly different curve, denoted as the meridional curve in fig. 1, it still passes through the zero and first order points discussed above, and its numerical deviation from the sagittal curve is small. In practice, one may use a flat detector operating at normal incidence to the ray diffracted from the grating pole without significant degradation of the resolution in either direction.

These theoretical results have been verified in a number of laboratory experiments. In fig. 2 I show spectra of a laser-produced aluminum plasma obtained using a prototype varied-space plane grating. The converging beam incident to this grating was produced by a multilayered spherical mirror operating near normal incidence. A flat film plane, oriented at normal incidence (i.e. "erect") to the zero order image, recorded well-defined stigmatic images over three octaves in wavelength. Theoretically, only a single wavelength (first order of 316 Å), was perfectly corrected by the varied-spacing. In practice the image sizes appeared to be dominated by the size of the plasma, used as the object point of the spectrometer in place of an entrance slit, rather than the aberrations of the optics. For example, the halos appearing around the Al IV 160.073 and 161.686 Å images are attributed to the expansion of the plasma over the time it required for these relatively low ionization states to cool. The microdensitometer trace shown in fig. 3 reveals that a spectral resolving power ($\lambda/\Delta\lambda$) of approximately 1000 is obtained near the correction wavelength).

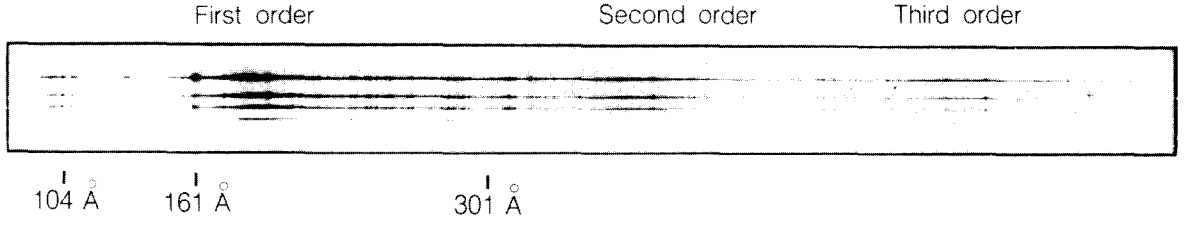

Fig. 2. Laboratory spectra obtained by focusing of a repetitively-pulsed Nd:YAG laser (1.064 μm wavelength) at a solid aluminum target. The plasma acted as the entrance slit of a spectrometer employing a varied-space plane grating in the convergent light provided by a molybdenum–silicon multilayered spherical mirror. A (flat) film plane was placed at normal incidence to the zero order beam, and astigmatism is seen to be absent over a wide range in wavelength in the extreme ultraviolet, while maintaining high spectral resolution. The different spectra correspond to different exposure times, the lowest being one laser shot (0.2 J). The multilayer provided maximum intensity near 200 Å wavelength, hence the appearance of Al V and Al VI lines near 100 Å are attributed to second order Bragg reflection by this mirror. The grating orders dispersed to different parts of the film are indicated at the top.

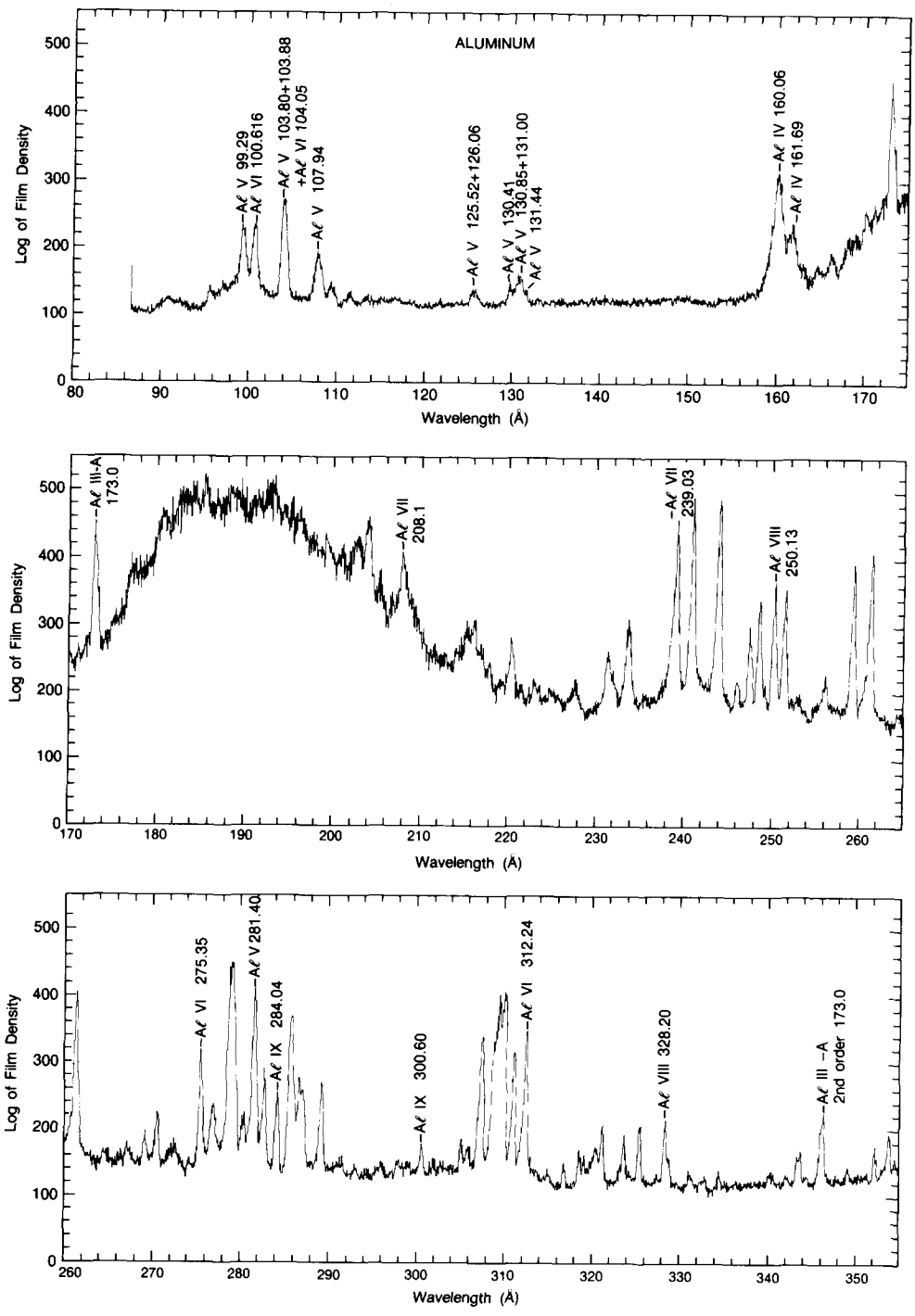

Fig. 3. Microdensitometer trace of a portion of one of the spectra shown in fig. 2. The broad appearance of the two Al IV lines near 160 Å is probably due to plasma expansion integrated over the exposure, as evidenced by the halos surrounding the 2-D images of these features in fig. 2. Measurement of the width of the unsaturated Al VI line at 312.24 Å indicates a spectral resolution of approximately 0.3 Å full-width-at-half-maximum.

The saturated portion of the spectra shown in figs. 2 and 3 near 200 Å is due to the high reflectance near the peak of the multilayered mirror (Mo–Si) mentioned above. This peak is reproduced in second and third grating orders. A few features seen near 100 Å therefore suggest that the multilayer is also reflecting near its

second order peak. The combination of spectral orders 1, 2 and 3 from the grating and Bragg orders 0, 1 and 2 from the multilayer result in a rich spectrum which unfortunately is not amenable to accurate deconvolution.

To overcome this limitation, the multilayered normal incidence spherical mirror was replaced by two conventional grating incidence spherical mirrors oriented perpendicular to each other as in a Kirkpatrick–Baez microscope [8]. The convergent beam reflected by this combination contained a broad range of wavelengths, extending well into the soft X-ray below 100 Å. Though the grating was designed for use at much longer wavelength, in the extreme ultraviolet, it was determined both theoretically (see section 4) and experimentally that a simple rotation of the grating about its central groove would maintain moderate spectral resolution across a broad band of soft X-ray wavelengths. As the images are still free of astigmatism, high sensitivity is obtained using film. In fig. 4 I show the results of such an experiment, where the soft X-ray spectrum is that of carbon from a single laser pulse focused at a graphite target. High sensitivity and high resolution spectra of plasmas at wavelengths below approximately 30 Å are of major importance to research in extragalactic astronomy [7]. The spectral region between the absorption K-shell edges of oxygen (23 Å) and carbon (45 Å) is also of special interest to current research topics in cell biology.

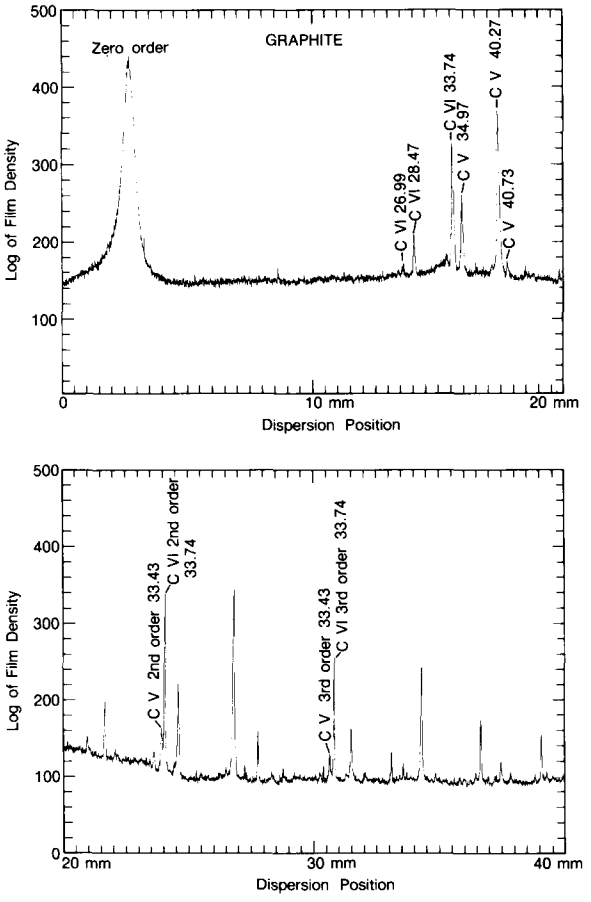

Fig. 4. Microdensitometer trace of a spectrum taken of a laser-produced graphite plasma, showing the soft X-ray line emission from carbon. The spectrometer employed two spherical mirrors oriented orthogonally to each other and at grazing incidence to the X-ray beam, to provide the convergent radiation to the same grating used to obtain the results of figs. 2 and 3. This grating, intended for best focusing at much longer wavelengths, was rotated about its central groove to direct this portion of the soft X-ray spectrum upon a fixed film plane. High spectral resolution is seen to be maintained by this simple wavelength selection procedure.

Another advantageous property of the grating geometry presented above is that the grating is plane and employs straight grooves. Since this prevents significant focusing along the lengths of the grooves, a large angular acceptance is permitted in that direction. The main aberration, sagittal coma, was found to limit the spectral resolving power [3,4] to $\lambda/\Delta\lambda = 8a_y^{-2}$, where a_y is the angular convergence, in rad, of the beam along the grooves. This proved particularly helpful in the design of spectrometers for space observatories [5,7], where the beam speed provided by large astronomical telescopes can be as large as 0.15 rad. In this case the varied-space plane grating will still yield resolving powers of 10^2–10^3, while in laboratory applications ($a_y = 0.010$–0.001 rad), resolving powers in excess of 10^4 are possible.

With the above theoretical and experimental background developed as a building block to the design of new geometries for grazing incidence optical systems employing gratings, I now turn to a review in sections 3 and 4 of two monochromator designs which have evolved from these considerations.

3. High throughput monochromator

This design arose out of the need for collection of a large solid angle from an isotropically emitting laboratory light source. Other requirements included a stigmatic image to provide maximum light intensity per unit area, a spectral resolving power of approximately 100, a disposable first optic to collect plasma debris from the light source and compatibility with ultrahigh vacuum.

Familiar designs such as the toroidal grating monochromator [9,10] were first investigated as stigmatic options. However, such gratings remove astigmatism by the sagittal focusing due to a highly curved surface along the lengths of the grating grooves, resulting in large geometrical aberrations (dominantly sagittal coma) which degrade the spectral resolution.

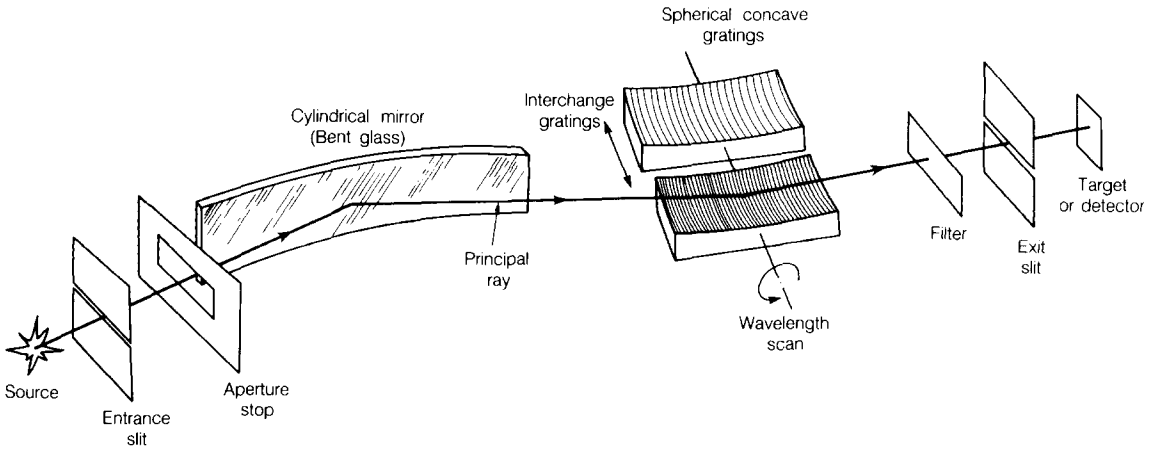

Fig. 5. Optical schematic of the high throughput monochromator (HTM). This design employs conventional spherical gratings, and a separate curved mirror to remove astigmatism. This simple design was devised as an alternative to the toroidal grating monochromator, for high solid angle acceptance and low to medium spectral resolution using fixed slits.

A clue to an improved high throughout design was the high collection ability along the groove lengths of the plane grating discussed in section 2, where the task of removing astigmatism is accomplished by a separate mirror preceding the grating. The requirement for only modest spectral resolution then encouraged a simplification whereby varied-spacing was unnecessary. The spectral focusing thus used a grating surface curved in the dispersion plane, incident light which diverged in that plane and equally-spaced grooves along the chord of the grating surface. This low resolution adaptation of the varied-spaced plane grating geometry theoretically implied a cylindrical grating, however, it was determined that a simple spherical grating recovered most of the improvement in throughput due to its small amount of sagittal focusing (fig. 5). Further simplifications which made it convenient to use such an instrument in ultrahigh vacuum were the use of fixed slits and wavelength selection by rotation of the grating about its central groove, maintaining fixed directions for the incoming and outgoing light. This high throughput monochromator (HTM) was determined experimentally [11] to provide intensities approximately two orders of magnitude higher than conventional laboratory monochromators.

A laser-produced plasma light source facility, at the Sandia National Laboratory, has used the HTM to obtain the highest intensities yet reported in the laboratory (excluding synchrotrons) over the 100–300 Å region. In fig. 6 is shown a spectrum with an average intensity of 5×10^8 photons per 1% bandwidth per laser pulse of duration 40 ns. The stigmatic image size was approximately 0.1 mm^2 at the exit slit of the monochromator. These results were obtained under ultrahigh vacuum, in preparation for the application of this instrument in studies of photoelectron and fluorescence spectroscopy. To maximize the count-rates per unit time, the laser can be run at 10 Hz with approximately the same power per pulse as the 1 Hz results displayed in fig. 6, resulting in peak intensities of 10^{10} photons/s/1% bandwidth/0.1 mm^2.

The author has used the HTM to feed monochromatic light to a vacuum reflectometer designed to measure efficiencies and scatter profiles of optical elements

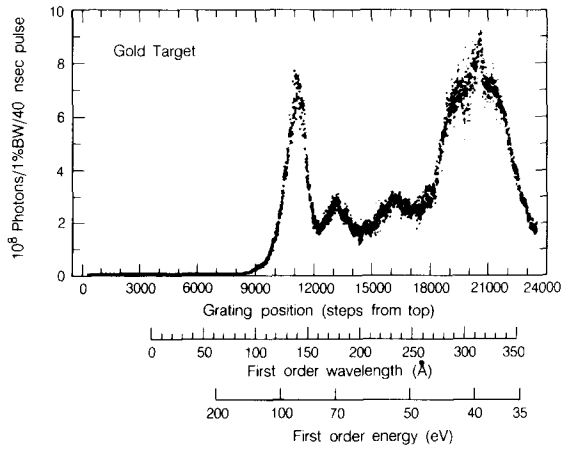

Fig. 6. Spectrum of a laser produced gold plasma obtained using the HTM at a resolving power of 100. A single pulse of a krypton fluoride laser (248 nm, 1 J, 40 ns duration) was used per data point. Wavelength was scanned through a fixed exit slit, and the astigmatism removal mirror inside the monochromator adjusted in radius to allow maximum throughput through the entrance slit of a double ion chamber detector. The efficiency of this detector was removed from the data. These intensities were obtained over a stigmatic image of approximately 0.1 mm^2. This figure courtesy of T. Tooman of the Sandia National Laboratory in Livermore, California.

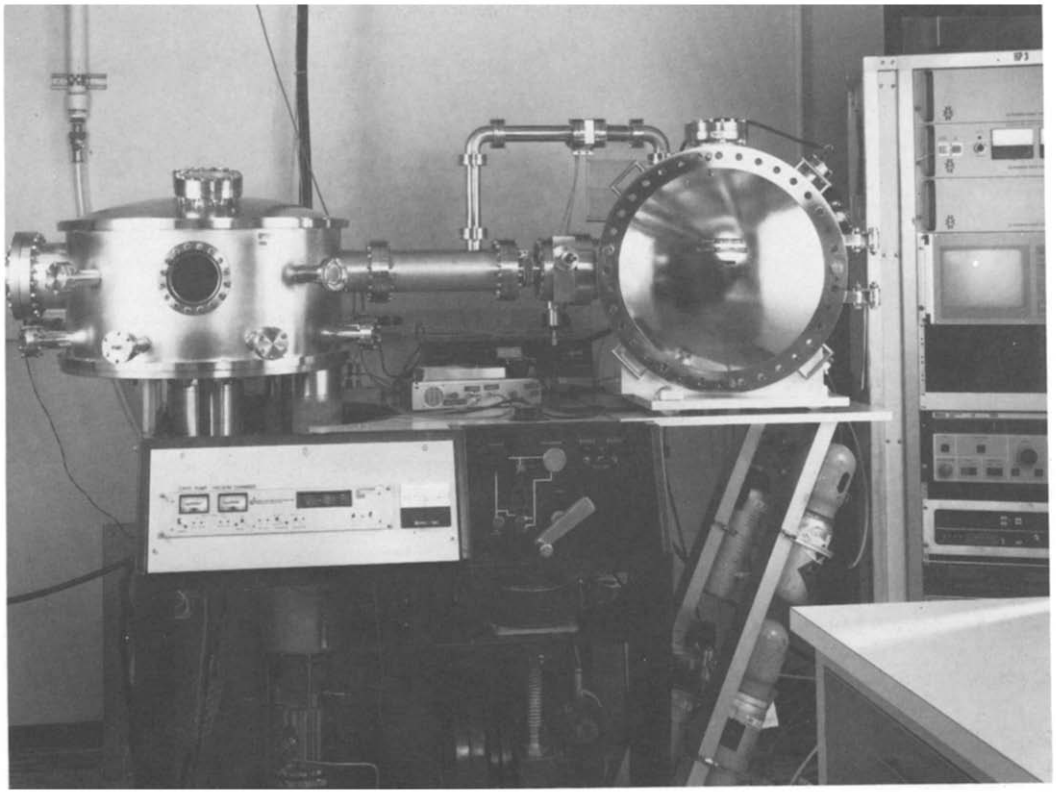

Fig. 7. Exterior of vacuum reflectometer, consisting of (from right to left), Penning light source (not shown), high throughput monochromator and dual-goniometer chamber at the Center for X-ray Optics in Berkeley, California.

at any angle of incidence. The exterior of this instrument is shown in fig. 7. The light originated from the continuous line discharge of a Penning sputtering source [12], which provided useable spectral lines over the 100–400 Å region [11]. In fig. 8 I show a reflection grating efficiency curve versus the angle of incidence (measured from the grating tangent) at a wavelength of 130 Å. Such measurements yield information on the shape of the grating grooves. The peak efficiency of 36% shown here represents nearly 100% of the theoretical value for perfectly formed blazed grooves, and the angular position of this peak indicates the blaze angle is approximately 3.2°. Such information is used as feedback during the actual fabrication of the grating, in order to obtain the desired efficiency response.

With slits and apertures open to maximum values, the strongest line (160 Å) provided approximately 2×10^6 counts/s, including the efficiency of a channeltron detector. After narrowing the apertures to provide good angular resolution, sufficient intensity was still present to allow the detection of intensities in the wings of the scattered profile of spectral orders from a test ruled grating. In fig. 9 I show the results of one such measurement, where the groove density was 1200 grooves/mm, the blaze angle approximately 1.9° and the angle of incidence 74.65° to provide maximum intensity in the first order image. The detector was preceded by a slit of angular width 0.11° in the dispersion plane, and this

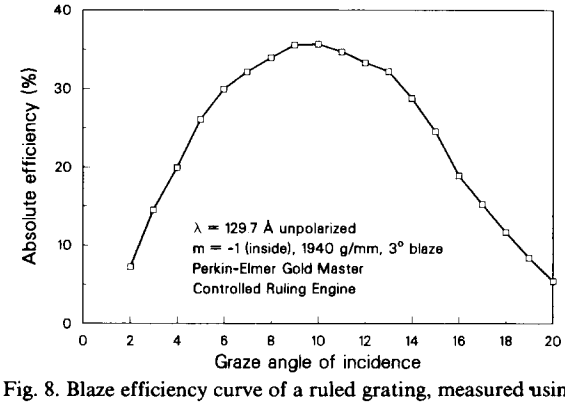

Fig. 8. Blaze efficiency curve of a ruled grating, measured using a vacuum reflectometer. A monochromator wavelength of 129.7 Å was selected by the HTM which fed this reflectometer. The light source was a Penning discharge lamp. This result provides a measure of the grating groove shape (e.g. the value of the blaze angle).

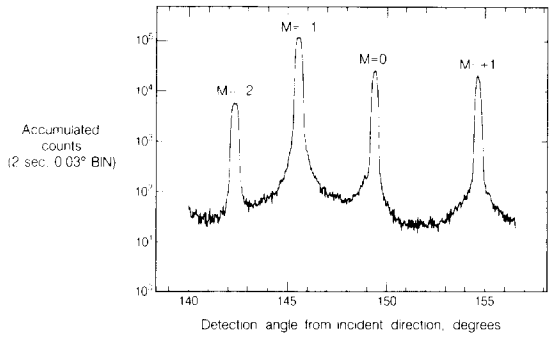

Fig. 9. Spectrum of a 1200 groove/mm ruled grating (supplied by G. Hirst and S. Coles of the Perkin–Elmer Corporation), when illuminated by a monochromatic wavelength near 161 Å. Spectral orders −2 through +1 were intercepted by a scanning detector/slit. After correction for geometrical effects, the efficiency in the blazed order (minus first) is measured to be 5.7 times higher than that in the zero order or plus first order. Between the minus first and zero orders the level of scattered in-plane light ("grass") is seen to be approximately a factor of 1500 lower than the first order peak, per angular bin of 0.11°. The noise due to detector background is approximately 1 count/s.

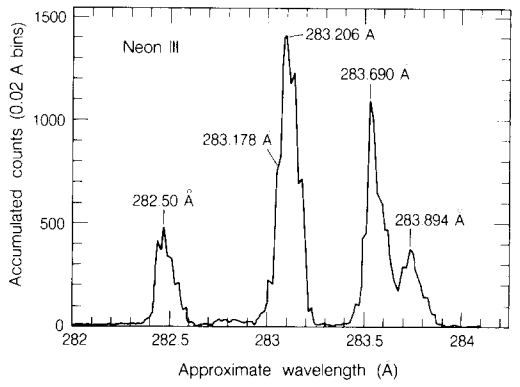

Fig. 10. High resolution spectrum of neon taken with an HTM using fixed slits. To obtain the resolution of 0.1 Å, the acceptance apertures of the monochromator needed to be severely narrowed. This spectrum required approximately one hour to scan.

combination was scanned point-by-point every 0.03° to construct the spectrum. The detector dark count rate was approximate 1 count/s, thus the intensities shown between the various spectral orders were due to actual scattered light. Midway between the first and zero orders, the scattered light level ("grass") is seen to be approximately a factor of 1500 lower than the first order peak. This converts to a scattered light level of 4.2×10^{-5} per ångström of the first order integrated intensity, which compares well with the best ruled or holographic gratings previous reported in the far ultraviolet [13].

As the apertures of the illuminated optics in the HTM were narrowed, an increase in spectral resolution became evident. In fig. 10 I show a high resolution spectrum of neon as a function of wavelength. Using fixed slits, the spherical grating suffers from considerable defocusing as wavelength is scanned away from two correction wavelengths. Because of this, the optimum grating aperture necessary to balance this geometrical aberration and the limit of physical diffraction, was small. Though a spectral resolving power of approximately 3000 is shown in fig. 10, such a measurement required over an hour of scanning due to the small geometrical acceptance.

Another practical limitation to the resolution obtained in the prototype HTM resulted from the use of a low quality bent glass mirror between the entrance and exit slits. Fortunately, due to the orientation of this mirror perpendicular to dispersion, the only slope errors which could degrade the spectral resolution are those in the sagittal direction of the mirror. Due to the use of grazing incidence, such slope errors are attenuated by the sine of the graze angle. This is because the image will be spread out along the circumference of a cone with half-angle equal to the graze angle, e.g. a 90° slope error will cause an actual angular deviation of twice the graze angle. However, it was still found that such errors required aperture-stopping this mirror to obtain resolving powers in excess of 1000. A solution to this problem is evident when one realizes that this astigmatism-control mirror can be positioned anywhere between the source and detector [11]. If intended for high resolution, this mirror could be placed prior to the entrance slit, which would act as a spatial filter to transmit only the well-focused central core or reflected beam. Moreover, a higher quality mirror would then serve to increase the fraction of the reflected light which passes through the entrance slit, while maintaining resolution limited by the slit width.

However, the HTM suffers from the more fundamental limitation of a grazing incidence focal surface, due to the spherical equally-spaced grating. As the grating is rotated about its central groove to scan wavelength, this focal curve deviates radically from the position of fixed slits. The only obvious technical fix to this problem involves a significant repositioning of the entrance or exit slit as a function of wavelength. In the next section I present an alternative to this, which allows the use of fixed slits yet maintains high spectral resolution at all wavelengths.

4. High resolution erect field spectrometer

The basic design discussed in section 2, employing a varied-space plane grating in combination with a

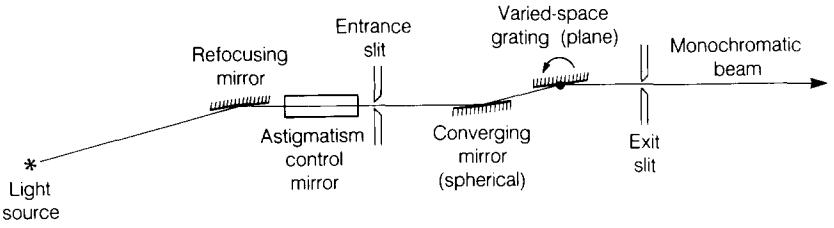

Fig. 11. Optical schematic of the high resolution erect field spectrometer (HIREFS). This design employs a high quality spherical mirror and plane grating combination between fixed position entrance and exit slits. The groove spacings on the grating surface are varied in such a way that optimum spectrum resolution is maintained as the grating is rotated (arrow) about its central groove to select wavelength. Control of astigmatism is accomplished by a separate mirror shown here prior to the entrance slit. This slit acts as a spatial filter to transmit only the central well-focused region of the refocused image.

spherical mirror to provide the required convergent beam incident to the grating, results in a focal surface nearly erect (i.e. at normal incidence) to the diffracted beam. This suggests that as such a grating is rotated, the focal surface may also rotate and distort slightly, but should remain at approximately the same focal distance from the grating. In section 2, experimental confirmation of this effect was presented (fig. 4). In a previous publication, this effect was examined in parametric form and it was determined that the varied-space function could be adjusted to optimize the spectral resolution through such a wavelength scan using fixed entrance slit and detector (or exit slit) [14]. This optical system, one embodiment of which is illustrated in fig. 11, is referred to by the author as HIREFS (high resolution erect field spectrometer (or monochromator)].

The essential reason why this may be done is due to the extra degree of freedom provided by varied-spacing. According to Fermat's principle, the equation which must be met in order to remove the dominant (linear) error in the ray aberration from a plane grating is a function of five quantities: the angle of incidence, the angle of diffraction, the object distance, the image distance and the linear term in space variation between the grooves. The first two of these are constrained by the grating equating for a specified included angle between the incident and diffracted beams and for a nominal groove spacing given a desired wavelength and spectral order. The image distance (the distance to the exit slit) is constrained by the desired plate scale. This leaves two quantities: the object distance and the linear varied-spacing term. Thus, the equation can be met at two wavelengths of choice, as in the case of the conventional grating HTM. However, due to the normal incidence focal surface from the plane varied-space grating, deviation from this analytic curve at intermediate wavelengths is small as the grating is rotated about its central groove to select wavelength. It is important to note that this property is not shared by concave gratings which are corrected holographically or mechanically to yield erect focal planes, due to the strong dependence of the focal length upon the angle of incidence [15].

This effect is clearly demonstrated in fig. 12 where a conventional spherical grating (HTM) and a varied-space plane grating (HIREFS) are compared for the same aperture, corresponding to 4 mrad diverging from the exist slit. Over two orders of magnitude improvement in resolution, resulting from a reduction in total geometrical aberration (Including terms of order higher than discussed above), is obtained in going to a varied-space grating. This improvement is so great that the HIREFS becomes diffraction limited at approximately 10^{-4} fractional wavelength resolution for this assumed fixed aperture.

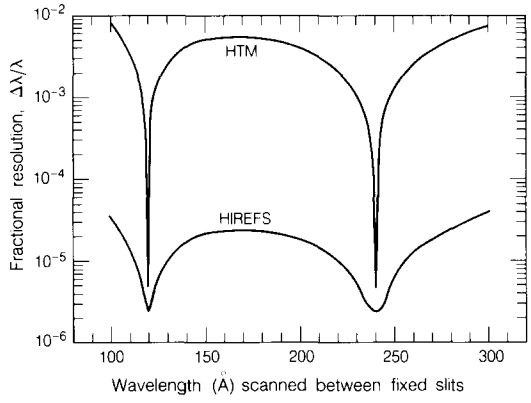

Fig. 12. Spectral resolution versus wavelength for the two stigmatic monochromator designs illustrated in figs. 5 and 11. Both designs select wavelength by a rotation of the grating about its central groove, use fixed slits at an included angle of 172°, a 300 groove/mm grating operating in the inside first order, a 681.5 mm distance between grating pole and exit slit, and a beam divergence of 4 mrad through the exit slit. Only geometrical aberrations are included. Diffraction due to the finite number of active grooves would limit the resolution to above approximately 10^{-4}. The erect field property of the varied-space plane grating in the HIREFS design results in little degradation of the resolution as the grating is rotated to scan wavelengths, whereas the degradation of the HTM design is severe due to the grazing incidence focal surface of a conventional spherical grating.

III(c). GRATING MONOCHROMATORS

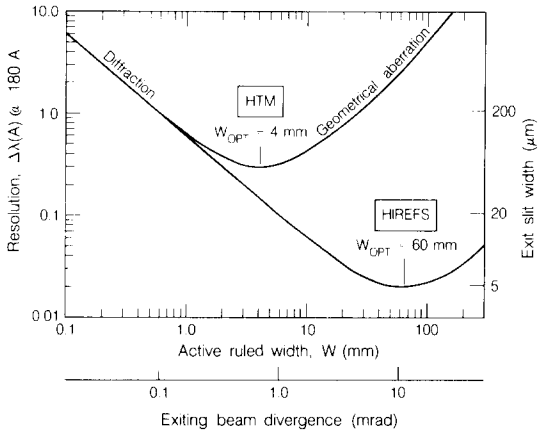

Fig. 13. Spectral resolution (extremum width) at a wavelength of 180 Å, as a function of the aperture in the dispersion plane for the two stigmatic monochromator designs illustrated in figs. 5 and 11. Both designs use fixed slits and yield minimum geometrical aberration at 120 and 240 Å, as shown in fig. 12. The optimum active ruled width, W_{opt}, is a compromise between a narrowing diffraction pattern and an increasing geometrical aberration as the aperture increases. Due to its smaller inherent geometrical aberration, the varied-space plane grating in the HIREFS design achieves both improved resolution (0.02 Å vs 0.4 Å) and higher acceptance (10 mrad vs 0.6 mrad) than the spherical grating HTM design.

Due to the difference in inherent geometrical aberration, a true maximization of the attainable spectral resolution requires that the optimum ruled width be found for the two designs. This is given in fig. 13, revealing a factor of 15 increase in both resolution and collecting aperture of the varied-space design.

Assuming an undulator light source [1] which provides a diffraction-limited beam, one would first use a premirror to adjust the source size as imaged onto the entrance slit of the monochromator. If the source size is demagnified by a factor P, then a corresponding increase P in the beam divergence results in order to conserve entropy. In optical nomenclature, the emittance of the light source is constant. As the factor P increases, the illuminated width of the grating increases. This improves the resolution resulting from the limit of physical diffraction, but degrades the resolution resulting from geometrical aberrations. Therefore, it is always possible to choose a premirror demagnification such that the monochromator will accept the entire emittance of the light source, and be equally limited by physical diffraction and by geometrical aberrations. This result is independent of the relative merit of one monochromator design versus another. In the present analysis, the HIREFS would achieve the factor 15 improvement over the HTM illustrated above if it used a premirror of demagnification 15 times greater than for which the HTM would be optimized.

The focal length assumed in constructing fig. 13 was small (681.5 mm) in comparison to the length available in most synchrotron radiation beamlines. The optimum aperture (e.g. 60 mm for the HIREFS) scales as the square root of the focal length, thus an improvement of approximately a factor of two in aperture and spectral resolution is realized with a grating focal length of 3 m. This corresponds to a ruled width of 120 mm, a beam divergence of approximately 5 mrad through the exit slit, an entrance slit width of 10 μm and spectral resolution of 0.01 Å at 180 Å (resolving power: 1.8×10^4). The results shown in fig. 13 are due to the extreme image envelope width, thus the actual resolvable full-width-at-half-maximum widths correspond to a resolving power approximately 50% higher, or 2.8×10^4. Over a 10 mrad aperture, a factor of two higher resolving power would be realized at 45 Å, using a 1200 grooves/mm grating, where the 4° grazing angle still provides reasonable reflectance. Alternatively, in the wavelength region above 100 Å, a graze angle of 10° is acceptable, resulting in a resolving power of approximately 3×10^4.

Apart from the use of fixed entrance and exit slits, and a fixed beam direction exiting the monochromator, other practical technical advantages to the HIREFS design include:

(i) The use of only plane and spherical optical surfaces as high resolution elements between the entrance and exit slits. These surfaces can be fabricated and tested to extremely high figure accuracy tolerances, providing the required diffraction-limited imaging performance in the soft X-ray.

(ii) The use of a straight and parallel grooved grating, permitting its fabrication by mechanical ruling engines.

(iii) The presence of an erect focal plane which allows a loose tolerance on the transverse placement of the exit slit (i.e. compared to placing an exit slit along a grazing incidence focal curve such as the Rowland circle).

In the foregoing discussion, one particular aberration was removed at two wavelengths of choice by exploiting a degree of freedom provided by varied spaced grooves. However, other higher order aberrations and derivatives of aberrations may also be removed in order to tailor the performance of a given optical system. This includes varying the groove spacings so as to remove aberrations caused by other optical elements in the system.

5. Conclusions

The following points are summarized from the foregoing discussions:

(A) A progression of stigmatic grazing incidence monochromator designs is evident, from toroidal grating monochromators (TGM) which use a minimum of

one optical surface, to designs which achieve higher performance by the separation of functions using multiple optics. These include the high throughput monochromator (HTM) which uses a minimum of two optical surfaces, to designs (HIREFS) employing varied-space plane gratings which use a minimum of three optical surfaces.

(B) The HTM design represents an improvement over the TGM design due to a large reduction in the amount of sagittal coma.

(C) The emittance of a light source may be matched with any monochromator design, regardless of its performance, by choosing a premirror magnification which equalizes the two competing effects of physical diffraction and geometrical aberrations.

(D) The HIREFS monochromator achieves both a higher spectral resolution and a larger collecting aperture than the HTM.

(E) The HIREFS design facilitates the kinematical design of (ultrahigh vacuum) synchrotron beamlines, as it utilizes fixed slits and a fixed beam direction for all wavelengths. This geometry also results in perfect correction of astigmatism at all wavelengths, due to an unchanging path length through the system.

(F) The HIREFS design is also of practical significance from a consideration of fabricating the optical elements, as it uses only plane and spherical surfaces, which can be figured to diffraction-limited performance in the soft X-ray. Because the grating grooves are straight and parallel, such varied-space gratings have been manufactured by mechanical ruling engines with efficiencies higher than holographic gratings, yet with an equally low level of scattered light.

(G) The HIREFS design provides an erect spectral field, useful in spectroscopic research, in addition to its use as a monochromator.

Acknowledgements

The author wishes to acknowledge that the results reported here in figs. 2, 3 and 4 were obtained in collaboration with Prof. S.M. Kahn, W. Craig and Prof. R.W. Falcone, all of the UC Berkeley Department of Physics, while working on a new research program initiated by SMK for the laboratory study of astrophysical plasma conditions. That work was supported in part by grants from the California Space Institute and by the Institute for Geophysics and Planetary Physics. I wish to thank T. Barbee for fabrication of the molybdenum–silicon multilayered mirror used in some of those experiments. The spherical replica grating employed in the high throughput monochromator (HTM) was fabricated by T. Harada of the Hitachi Central Research Laboratory, and used a new bakeable epoxy permitting its use in ultra-high vacuum. I also would like to acknowledge that the result reported here in fig. 6 was obtained at a new laser plasma facility developed at Sandia National Laboratory by T. Tooman. The author thanks G. Hirst and S. Coles of the Perkin–Elmer Corporation for their diligent efforts in producing the gratings whose results appear in figs. 8 and 9. I also benefited from discussions of scientific applications with Prof. F. Cerrina of the University of Wisconsin at Madison. Finally, I gratefully thank J.H. Underwood for many helpful discussions and joint efforts, D.T. Attwood for support and encouragement and P. Batson for excellent engineering work on the reflectometer, all from the Center for X-ray Optics at the Lawrence Berkeley Laboratory. This work was supported in part by the Department of Energy under contract No. DE-AC03-76SF00098.

References

[1] D. Attwood, K. Halbach and K.-Je Kim, Science 228 (1985) 1265.
[2] E.M. Rowe, Proc. 1987 Particle Accel. Conf., IEEE Catalog No. 87CH2387-9, p. 391.
[3] M.C. Hettrick and S. Bowyer, Appl. Opt. 22 (1983) 3921.
[4] M.C. Hettrick, Appl. Opt. 23 (1984) 3221.
[5] M.C. Hettrick et al., Appl. Opt. 24 (1985) 1737.
[6] M.C. Hettrick, Proc. Soc. Photo-Opt. Instr. Eng. 560 (1985) 96.
[7] M.C. Hettrick and S.M. Kahn, Proc. Soc. Photo-Opt. Instr. Eng. 597 (1985) 291.
[8] P. Kirkpatrick and A.V. Baez Jr., J. Opt. Soc. Am. 38 (1948) 766.
[9] W.R. McKinney and M.R. Howells, Nucl. Instr. and Meth. 172 (1980) 149.
[10] C.T. Chen, E.W. Plummer and M.R. Howells, Nucl. Instr. and Meth. 222 (1984) 103.
[11] M.C. Hettrick and J.H. Underwood, Appl. Opt. 25 (1986) 4231.
[12] D.S. Finley, S. Bowyer, F. Paresce and R.F. Malina, Appl. Opt. 18 (1979) 649.
[13] G.H. Mount and W.G. Fastie, Appl. Opt. 17 (1979) 3108.
[14] M.C. Hettrick and J.H. Underwood, AIP Conf. Proc. No. 147 (1986) 237.
[15] T. Kita, T. Harada, N. Nakano and H. Kuroda, Appl. Opt. 22 (1983) 512.